Molecular Human Reproduction, Vol.26, No.6, pp. 389–401, 2020
Advance Access Publication on April 24, 2020 doi:10.1093/molehr/gaaa027

molecular human reproduction

ORIGINAL RESEARCH

Deficiency of the onco-miRNA cluster, *miR-106b∼25*, causes oligozoospermia and the cooperative action of *miR-106b∼25* and *miR-17∼92* is required to maintain male fertility

Alicia Hurtado[1], Rogelio Palomino[2], Ina Georg[3], Miguel Lao[1], Francisca M. Real[4], F. David Carmona [1], Miguel Burgos[1], Rafael Jiménez [1,*], and Francisco J. Barrionuevo[1]

[1]Departamento de Genética e Instituto de Biotecnología, Universidad de Granada, Labs 127 and 105a, Centro de Investigación Biomédica, Avenida del Conocimiento, 18016 Armilla, Granada, Spain; [2]Departamento de Bioquímica y Biología Molecular I e Instituto de Investigación Biosanitaria de Granada, Universidad de Granada, Laboratorio 127 Centro de Investigación Biomédica, Avenida del Conocimiento, 18016 Armilla, Granada, Spain; [3]Genetics of Complex Diseases Unit, Pfizer-University of Granada-Junta de Andalucía "Centre for Genomics and Oncological Research" (GENYO), Avenida de la Ilustración 114, 18016 Granada, Spain; [4]Present address: Max Planck Institute for Molecular Genetics, Research Group Mundlos, Ihnestrasse 73, D-14195 Berlin, Germany

*Correspondence address. Departamento de Genética e Instituto de Biotecnología, Universidad de Granada, Labs 127 and 105a, Centro de Investigación Biomédica, Avenida del Conocimiento, 18016 Armilla, Granada, Spain. Tel: +34-958243260; E-mail: rjimenez@ugr.es
https://orcid.org/0000-0003-4103-8219

Submitted on November 29, 2019; resubmitted on March 27, 2020; editorial decision on April 14, 2020

ABSTRACT: The identification of new genes involved in sexual development and gonadal function as potential candidates causing male infertility is important for both diagnostic and therapeutic purposes. Deficiency of the onco-miRNA cluster *miR-17∼92* has been shown to disrupt spermatogenesis, whereas mutations in its paralog cluster, *miR-106b∼25*, that is expressed in the same cells, were reported to have no effect on testis development and function. The aim of this work is to determine the role of these two miRNA clusters in spermatogenesis and male fertility. For this, we analyzed *miR-106b∼25* and *miR-17∼92* single and double mouse mutants and compared them to control mice. We found that *miR-106b∼25* knock out testes show reduced size, oligozoospermia and altered spermatogenesis. Transcriptomic analysis showed that multiple molecular pathways are deregulated in these mutant testes. Nevertheless, mutant males conserved normal fertility even when early spermatogenesis and other functions were disrupted. In contrast, *miR-17∼92*$^{+/-}$*; miR-106b∼25*$^{-/-}$ double mutants showed severely disrupted testicular histology and significantly reduced fertility. Our results indicate that *miR-106b∼25* and *miR-17∼92* ensure accurate gene expression levels in the adult testis, keeping them within the required thresholds. They play a crucial role in testis homeostasis and are required to maintain male fertility. Hence, we have identified new candidate genetic factors to be screened in the molecular diagnosis of human males with reproductive disorders. Finally, considering the well-known oncogenic nature of these two clusters and the fact that patients with reduced fertility are more prone to testicular cancer, our results might also help to elucidate the molecular mechanisms linking both pathologies.

Key words: microRNA / *miR-17∼92* / *miR-106b∼25* / onco-miRNA / oligozoospermia / male infertility

Introduction

Human male infertility is frequently associated to disorders/differences of sex development (DSD), which are relatively rare congenital conditions in which the development of chromosomal, gonadal and/or anatomic sex is atypical (Lee et al., 2006). Even though our knowledge of the genes and molecular pathways involved in mammalian sex determination and differentiation has been significantly improved in recent years, it is estimated that only a small fraction of the DSD patients receive a precise molecular diagnosis, and that many DSD-causative genes remain unknown (Lee et al., 2016). Thus, the identification of new genes involved in sexual development and gonadal function as potential candidates for DSD is important for both diagnostic and therapeutic purposes.

MicroRNAs (miRNAs) are small regulatory RNA molecules able to either cleave or translationally repress their target mRNAs (Bartel, 2004). They are involved in the control of diverse genetic networks that affect many physiological processes, including development, differentiation, metabolism and cancer (Zhang et al., 2007). In some cases, miRNAs are grouped into clusters and transcribed as polycistronic transcripts. The *miR-17∼92* cluster (also called *Mirc1* in the mouse) includes six members (*miR-17*, *miR-18a*, *miR-19a*, *miR-20a*, *miR-19b-1* and *miR-92-1*) that are highly conserved in vertebrates and expressed in almost all tissues studied during pre- and postnatal stages (Ventura et al., 2008). Hemizygous deletion of human *MIR17HG* (the *miR-17∼92* host gene) causes the Feingold syndrome, an autosomal dominant condition characterized by multiple skeletal abnormalities (de Pontual et al., 2011). The *miR-17∼92* cluster is associated with several types of both hematopoietic and solid tumor cancers (Mogilyansky and Rigoutsos, 2013). Two paralog clusters exist in both the human and the mouse genomes, the *miR-106a∼363* cluster (*Mirc2*), which comprises six miRNAs (*miR-106a*, *miR-18b*, *miR-20b*, *miR-19b-2*, *miR-92a-2* and *miR-363*), and *miR-106b∼25* (*Mirc3*), with three members (*miR-106b*, *miR-93* and *miR-25*). The miRNAs of both *miR-17∼92* and *miR-106b∼25* have similar expression patterns in most tissues, whereas those of the *miR-106a-363* cluster are rarely expressed (Ventura et al., 2008). Like *miR-17∼92*, *miR-106b∼25* has been associated with different types of cancer, including breast (Guarnieri et al., 2018), liver (Li et al., 2009), lung (Lo Sardo et al., 2017), stomach (Zhang et al., 2014), prostate (Hudson et al., 2013), kidney (Xiang et al., 2015) and ovarian cancer (Zhu, 2012), among others.

Many studies have reported expression of the members of *miR-106b∼25* during the embryonic and postnatal development of primordial germ cells and at early stages of spermatogenesis (Hayashi et al., 2008; Niu et al., 2011; McIver et al., 2012; Smorag et al., 2012; Tong et al., 2012; He et al., 2013; Tan et al., 2014; Bhin, Jinhyuk et al., 2015; Hilz et al., 2017). Also, several studies have shown that *miR-106b∼25* is mis-expressed in patients with testicular anomalies, *miR-25* and *miR-93* being downregulated in testicular biopsies from patients with Sertoli cell only syndrome (Abu-Halima et al., 2014; Cheng et al., 2017). Similarly, the expression of *miR-93* was downregulated in the seminal plasma of oligoasthenozoospermic subfertile men (Abu-Halima et al., 2016), as well as in the testicular tissue of patients with non-obstructive azoospermia (Lian et al., 2009), and reduced expression of *miR-106b* seen in family members has been associated with human testicular cancer (Koster et al., 2010). In contrast, *miR-106b* was upregulated in the seminal plasma of both azoospermic and asthenozoospermic patients (Wang et al., 2011). Nevertheless, mice with a deletion of *miR-106b∼25* were reported to be viable and fertile and showed no obvious phenotypic abnormalities (Ventura et al., 2008). Thus, prompted by the large number of studies showing expression of *miR-106b∼25* and *miR-17∼92* during testicular development and its involvement in reproductive diseases, we decided to perform a more detailed study of the testicular features and fertility in mice carrying both single and double mutations of these clusters.

Materials and methods

Mice

miR-106b∼25 null mutants and *miR-17∼92flox/flox* control mice, both on a C57BL/6 × 129S4/SvJae genetic background, were obtained from the Jackson Laboratory (Bar Harbor, ME, USA; Stocks No: 008460 and 008458, respectively). To generate *miR-106b∼25*$^{-/-}$;*miR-17∼92*$^{+/-}$ mutant mice, *miR-17∼92*$^{flox/flox}$ mice were crossed to CAG-Cre mice (Belteki, 2005), and the resulting *miR-17∼92*$^{+/-}$ offspring were crossed to *miR-106b∼25*$^{-/-}$ mice to generate compound double heterozygotes: the latter mice were back-crossed to *miR-106b∼25*$^{-/-}$ mice to produce *miR-106b∼25*$^{-/-}$;*miR-17∼92*$^{+/-}$ mice. All animal experiments in this study were approved by the University of Granada Ethics Committee for Animal Experimentation (exp. No: 2011–341), and performed in accordance with the relevant guidelines and regulations dictated by this Committee.

Male fertility tests

Three control and three mutant males at postnatal day 60 (P60) were mated separately with two P60 control females each for a period of 5 months and the size and the number of the resulting litters were recorded.

Histological and immunohistological methods

Gonads were dissected out, weighed and prepared for standard histological methods, including hematoxylin and eosin staining. Testes were transversally sectioned to obtain cross sections of most seminiferous tubules. To assess the spermatogenesis condition, Johnsen's scores were determined. For this, 100 different seminiferous tubules were analyzed in each individual. Every tubular section was given a score ranging from 1 to 10 according to the most mature germ cells present in it (Johnsen, 1970). Also, single and double immunofluorescence analysis was performed, as previously described (Dadhich et al., 2013). We studied the spatial expression pattern of the following proteins: Laminin (a principal component of the basement membrane), Claudin11 (a transmembrane protein of the tight juntncions that form blood-testis barrier [BTB]), MNCD2 (N-Cadherin) (a component of the adherents junctions and ectoplasmic specialization formed in Sertoli-Sertoli and Sertoli-germ cell interactions), DMC1 (a recombination protein present from leptotene to early pachytene spermatocytes), PCNA (proliferating cell nuclear antigen present in both spermatogonia and zygotene-pachytene spermatocytes), and Ubiquitin (involved in protein degradation). Supplementary Table SI summarizes the antibodies used.

Analysis of BTB permeability

To test the permeability of the BTB in the testes of control and mutant mice we used a biotin-labeled tracer compound [EZ-Link Sulfo-NHS-LC-Biotin tracer, Thermo Scientific (Waltham, MA, USA)] as described (Dadhich *et al.*, 2013). Briefly, mice were anasthesized by halothane inhalation, their testes were exposed, and 50 µl of the tracer solution was placed beneath the tunica albuginea of the left testis, injecting at several points. The right testis was also treated in a similar way, but only PBS with 1 mM CaCl2 was injected, as a control. The testes were placed again inside the body of the mice, and 30 min later they were euthanized. The testes were then dissected out and fixed overnight in 4% formaldehyde. Testes were dehydrated, embedded in paraffin (Paraplast plus from Leyca Biosystems, Wetzlar, Germany) and sectioned (5 µm thick) according to standard procedures. Histological preparations were dewaxed and rehydrated and the tracer was detected by incubating the sections for 30 min with an Alexa Fluor 568-conjugated streptavidin solution (included in the tracer kit) at 25°C. To detect both the tracer and claudin 11, immunofluorescence for claudin 11 was performed before the tracer-detection technique was applied. Sections were then rinsed twice with PBS for 10 min, stained with DAPI (Sigma-Aldrich, Saint Louis, MO, USA), rinsed four additional times with PBS (20 min each), and mounted in Vectashield medium (Vector Labs. Burlingame, California).

Analysis of apoptosis

To detect apoptotic cells we used the terminal deoxynucleotidyl transferase (TdT)-mediated dUTP nick end labeling (TUNEL) technology, using an *in situ* cell-death detection kit (Roche, Basel, Switzerland) according to the manufacturer's instructions. Briefly, 50 µl of the TUNEL reaction mixture were placed on dewaxed and rehydrated tissue preparations, covered with parafilm and incubated for 60 min at 37°C in a humidified atmosphere in the dark and rinsed in PBS. After being rinsed with PBS, preparations were treated with DAPI, mounted in Vectashield and observed under a fluorescence microscope (Nikon, Tokio, Japan) at 488-nm wavelength (green).

Testis transcriptome

Total RNA was isolated from the testes of three *miR-106b∼25*$^{-/-}$ and three control (*miR-17∼92*$^{flox/flox}$) mice at P60 using the Qiagen RNeasy Midi kit (Hilden, Germany) according to the manufacturer's instructions. Subsequently, the six samples were sent to Macrogen Inc. (Seoul, South Korea). After passing a quality check, libraries were prepared using a TrueSeq RNA Sample Prep Kit V2 (Illumina, San Diego, CA, USA) and they were paired-end sequenced separately in an Illumina HiSeq 4000 platform. The ArrayExpress accession number for these transcriptomes is E-MTAB-8964.

Bioinformatics

The RNA-seq reads (around 100 base in length) were mapped to the NCBI GRCm38 mouse genome and counted with the *align* and *featureCounts* function from the R subread package (Liao *et al.*, 2019). The number of reads varied from 42 to 57 million and from 60 to 67 million in the control and mutant samples, respectively. Successfully assigned alignment varied from 35 to 46 million (more than 85%) and from 46 to 55 million reads (more than 82%) in the control and mutant samples, respectively. Only genes with 1 or more cpm (counts per million) in at least two of the samples were considered to be expressed and were used for further analysis. Analysis of differential gene expression was performed with edgeR (Robinson *et al.*, 2010). The total number of reads per sample was normalized with the calcNormFactors function of edgeR. Gene Ontology analysis was performed for differentially expressed genes (false discovery rate (FDR) <0.001) using the *Database for Annotation, Visualization and Integrated Discovery* (DAVID) (Huang *et al.*, 2007). To identify alternative splicing (AS) changes, reads were mapped with OLego (Wu *et al.*, 2013) and subsequently the Quantas pipeline was used to infer transcript structure and quantify AS (Yan *et al.*, 2015). To visualize splice junctions, RNA-seq reads were mapped to the NCBI GRCm38 mouse genome with the subjunc function from the Rsubread package (Liao *et al.*, 2019), and Sashimi plots were generated with the Integrative Genome Viewers (Robinson *et al.*, 2011). Prediction of target sites for the two *miR-106b∼25* seed families was done using TargetScan (version 7.1) (Agarwal *et al.*, 2015). Protein–Protein interaction (PPI) analysis was performed using the STRING database (Szklarczyk *et al.*, 2019) and the Cytoscape software platform (Shannon, 2003).

Epididymal sperm counts

The two entire epididymides of each mouse were dissected out, placed in a small Petri dish containing 2 ml PBS and minced with a scalpel into pieces of 1–2 mm. Then, the whole content of the Petri dish was transferred to a 15 ml falcon tube and filled with more PBS to reach a volume of 5 ml. The sperm was expelled out of the epididymis fragments by gently pressing them against the tube wall with the conical end of a Kimble tissue grinder (Ref. 749515-1500; Kimble Chase, Meiningen, Germany). The sperm suspension was allowed to stand for 1 min and 100 µl were taken from the upper clean part and further diluted 30–50 times (depending on the initial sperm concentration) with PBS before counting in a Neubauer chamber (Brand, Wertheim Germany). Results are given as the total number of sperm per mouse.

Serum testosterone measurements

Control and *miR-106b∼25* knock out (KO) mice at P60 (five of each genotype) were euthanized and their peripheral blood immediately taken by heart puncture. Total serum testosterone concentrations were measured by quantitative immunofluorescence using the testosterone-specific kit of the *iCroma TM Reader* system (Boditech Med Inc. Chungcheon, South Korea), according to the manufacturer instructions.

Ubiquitination assay

HEK293T cells were cultured in 24-well plates (2.5×104 cells per well) and transiently transfected with *miR-106b* mimic, *miR-93* mimic or a negative control miRNA mimic (Dharmacon) at 0, 10, 25, 50 and 75 mM using INTERFERin® in vitro siRNA/miRNA transfection reagent (Polyplus-transfection). At 48 h after transfection, cells were harvested, lysed and analyzed by western blotting using an anti-ubiquitin antibody.

Statistical analysis

Data are reported as mean ± SD values. All groups of values fit a normal distribution, so we used Student's *t*-tests to compare the respective means using the free software *gnumeric* (developed by the GNOME Project). Differences between means were considered significant when $P < 0.05$.

Results

miR-106b∼25 KO mouse testes show reduced size, oligozoospermia and altered spermatogenesis

To study the role of the *miR-106b∼25* cluster during testis development and function we used a previously generated null mutant mouse strain in which the cluster was deleted from the 13th intron of its host gene, *Mcm7* (Ventura *et al.*, 2008) without altering its expression and splicing (we confirmed this in our RNA-seq study; Supplementary Table SII and Fig. S1). At P60, *miR-106b∼25*$^{-/-}$ mice presented a significant 30% reduction in the testis mass compared to controls (Fig. 1A; Supplementary Table SIII). However, as *miR-106b∼25*$^{-/-}$ mice were smaller than controls (Supplementary Table SIII), we also calculated the relative testis mass, expressed as a percentage of body mass, and confirmed a significant reduction in testis mass in the mutants (Fig. 1B; Supplementary Table SIII). We also determined the Johnsen's score, as it is a widely accepted, histologically quantitative method to check the spermatogenesis condition (Johnsen, 1970). The average Johnsen's scores (JS) was 8.8 in control (Fig. 1C and F), and 7.9 in mutant mice (Fig. 1C and G–I; Supplementary Table SIII). The mutant mice contained a majority of normal tubules (JS = 9–10; Fig. 1C and G) but also tubules with lower JS values (Fig. 1C and H), including some with JS < 4, which were absent in controls (Fig. 1C and I). Consistently, epididymal sperm counts were reduced (40%) in mutant mice compared to controls (Fig. 1D; Supplementary Table SIII). Finally, we checked whether the phenotype of the *miR-106b∼25* mutant mice could be associated with reduced testosterone production, but no difference in serum testosterone levels was found compared to controls (Fig. 1E; Supplementary Table SIII). Consistent with this, the relative seminal vesicle mass, (seminal vesicle mass/body mass × 100) showed no difference between the mutant and control condition (Supplementary Fig. S2 and Supplementary Table SIII). Our results therefore show that *miR-106b∼25* deficiency induces oligozoospermia in the mouse.

Multiple molecular pathways are deregulated in *miR-106b∼25* KO mouse testes

To shed light on the molecular mechanisms underlying the spermatogenic alterations observed in *miR-106b∼25* KO mice, we used RNA-seq to identify differentially expressed genes (DEG) when comparing mutant and control testes at P60. Initially, we analyzed the differences between the expression profiles of mutant and control samples using a hierarchical clustering analysis. As expected, replicate samples from the same condition clustered together, showing that the testis transcriptome is significantly and consistently affected when *miR-106b∼25* is absent (Fig. 2A). We found 2409 deregulated genes [*P* adjusted (FDR) < 0.001], 1130 being upregulated and 1279 downregulated (Supplementary Table SII). The smear plot, representing the logFC of the expression against the average expression, showed that most genes were deregulated by less than two-fold (Fig. 2B). Functional annotation clustering of DEG revealed a significant enrichment (Padj. < 0.05) in clusters related to cell division and mitosis, ubiquitination, DNA repair, cell–cell adhesion, mRNA splicing and extracellular matrix (Fig. 2C; Supplementary Table SIV). PPI analysis of DEG resulted in a large interaction network that included several subnetworks individually enriched in one of the previously identified categories (Fig. 2D; Supplementary Table SV). Depending on their target sequence, the individual members of *miR-106b∼25* can be grouped into two seed families, with *miR-93* and *miR-106* belonging to one family and *miR-25* to the other (Mogilyansky and Rigoutsos, 2013). As miRNA deletion typically results in the upregulation of predicted targets, we looked for genes upregulated in *miR-106b∼25* deficient testes and containing predicted binding sites for both seed families in their 3′ UTRs. We identified 25 and 13 genes for the *miR-106b/93* and *miR-25* seed families, respectively (Supplementary Table SVI). We also located these target genes in our PPI network, highlighted their direct interactions with other proteins, and observed that they were widely distributed throughout all subnetworks (Fig. 2E). These results indicate that the slight alteration in the expression levels of a multitude of genes in mutant testes is the result of direct deregulation of several genes carrying functional targets for the *miR-106b∼25* miRNAs that subsequently alters the expression of many other genes with which they directly interact at the molecular level.

Early spermatogenesis and other functions are disrupted in *miR-106b∼25* KO mouse testes

Cell division is an important biological process affected in *miR-106b∼25* KO testes (Fig. 2C), and spermatogenesis includes both mitotic and meiotic divisions. To uncover stage-specific gene deregulation in *miR-106b∼25* KO testes, we used the recently published gene expression signature of the 14 spermatogenic clusters identified by Hermann *et al.* (2018), using single-cell RNA-seq technology. We identified which genes among those deregulated in *miR-106b∼25* KO testes are known to be expressed in specific cell types, and found that the stages with highest number of deregulated genes corresponded to those of early spermatogenesis, from undifferentiated spermatogonia to leptotene-zygotene spermatocytes (Fig. 3A; Supplementary Table SVII), coinciding with the stages where members of the *miR-106b∼25* cluster are expressed. Interestingly, at these early stages, downregulated genes were the most abundant. Also, we studied by immunofluorescence the expression patterns of two germ cell markers, namely PCNA, expressed in mitotic spermatogonia as well as in zygotene and pachytene spermatocytes (Steger, 1998), and meiotic recombination protein (DMC1), a marker for leptotene-to-early pachytene spermatocytes (Yoshida *et al.*, 1998). A similar expression pattern was observed in both mutant and control testes of P60 mice for both PCNA (Fig. 3B, D, E and G) and DMC1 (Fig. 3C, D, F and G). However, the percentage of DMC1^{+} tubules was significantly increased (40%) in the *miR-106b∼25* KO testes compared to controls (Fig. 3H; Supplementary Table SIII). These results show that slight deregulation

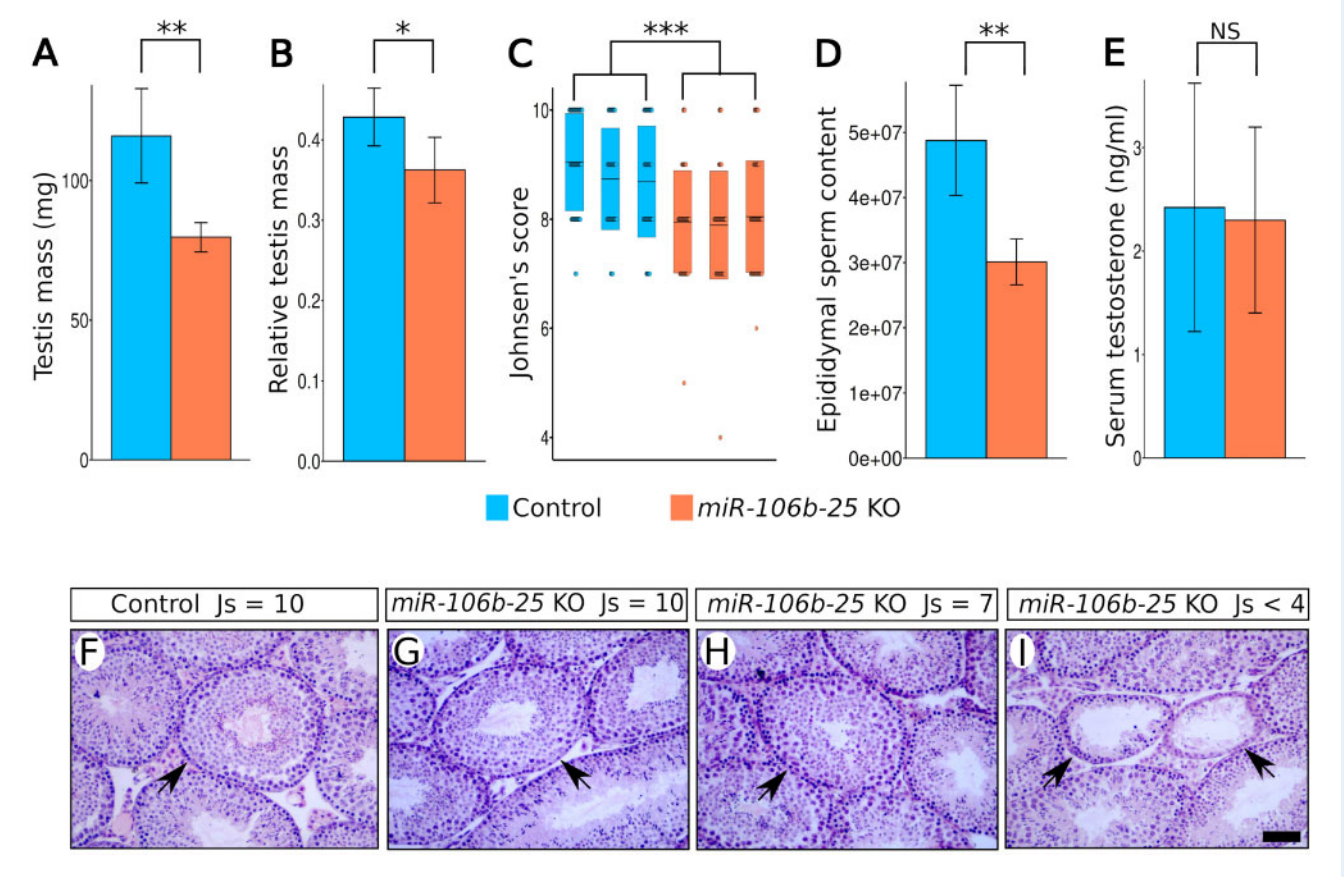

Figure 1 Testicular phenotype and fertility of microRNA *miR-106b~25* KO mice compared with controls at P60. (**A**) Testis mass. (**B**) Relative testis mass calculated as: testis mass (g)/body mass (g) × 100. (**C**) Johnsen's scores of three control and three *miR-106b~25* deficient testes. (**D**) Epididymal sperm counts. (**E**) Total serum testosterone concentrations. (**F–I**) Hematoxilin and eosin-stained histological sections of control (F) and mutant (G–I) testes, with indication of the Johnsen's scores (JS) corresponding to the tubular sections marked with arrows. Bars in (A–E) represent mean ± SD. Statistical significance of the differences between mean values was determined using Student's *t*-tests; $n = 10$ (5 control and 5 *miR-106b~25* KO mice) in A, B, D and E; $n = 6$ (3 control and 3 *miR-106b~25* KO mice) in (C). All numeric data are included in Supplementary Table SIII. Scale bar shown in I represents 50 μm in all micrographs. KO, knock out.

of a high number of genes during early spermatogenesis in *miR-106b~25* KO testes leads to a delay of the cycle at these stages.

Sertoli-Sertoli and Sertoli-germ cell adhesions are necessary for the correct progression of the spermatogenic cycle (Lui and Cheng, 2013) and we found that cell adhesion is one of the biological processes altered in *miR-106b~25* KO testes (Fig. 2C; Supplementary Table SIV). We also studied by immunofluorescence the expression of N-cadherin, present in the ectoplasmic specializations existing in both Sertoli-Sertoli and Sertoli-germ cell contacts, and claudin 11, a main component of the BTB. No differences were observed between control and mutant testes at P60 in the expression pattern of both proteins (Supplementary Fig. S3A–C and F). Furthermore, the injection of a biotin-labeled tracer showed that the BTB was functional (impermeable) in both *miR-106b~25* KO and control testes (Supplementary Fig. S3D, E, G and H). Moreover, although some extracellular matrix genes appeared altered in our transcriptome analysis, the expression pattern of laminin, a major component of the basement membrane, remained unchanged in mutant testes (Supplementary Fig. S3I and J). These results show that mild deregulation of cell adhesion and extracellular matrix genes does not appear to disrupt the assembly of these structures.

Using a TUNEL assay, we observed that *miR-106b~25* KO testes do not undergo increased apoptosis. The number of positive cells was very low (Supplementary Fig. S3L and M) in both control and mutant testes at P60, suggesting that cell death is probably irrelevant to the alterations observed in the mutant gonads.

Another biological process affected in mutant testes was ubiquitination (Fig. 2C; Supplementary Table SIV). We checked whether these miRNAs could affect ubiquitination *in vitro* by transfecting HEK293 cells with increasing concentrations of *miR-93* and *miR-106b* miRNA mimics and checking the status of conjugated ubiquitin by western blotting. However, no differences were detected between control and miRNA-mimic-transfected cells (Supplementary Fig. S4), showing that the absence of these miRNAs appears not to affect ubiquitination at detectable levels.

Our transcriptomic analysis also revealed that mRNA splicing was another functional category affected in mutant testes (Fig. 2C;

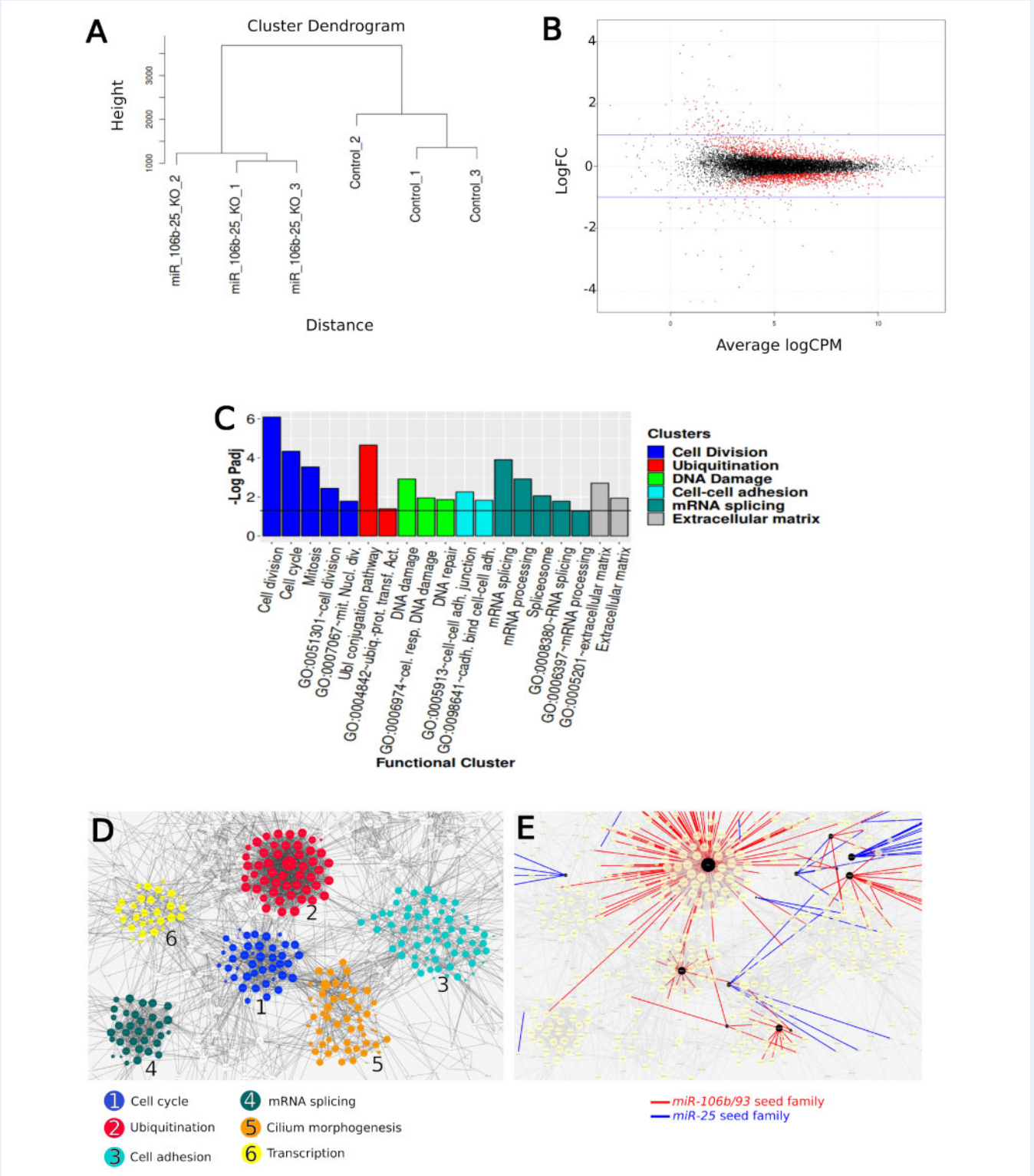

Figure 2 Bioinformatics analysis of RNA-seq data from *miR-106b~25* KO and control testes at P60. (**A**) Hierarchical clustering analysis showing that replicate samples from the same condition cluster together. (**B**) Smear plot to visualize the differential expression amplitudes; genes showing a statistically significant deviation are represented with red dots, the rest (black dots) being not significant. Note that most differentially expressed genes change in expression by less than 2-fold (Log fold-change = 1; blue lines). (**C**) Functional annotation clustering of DEG showing enrichment in six important biological processes. (**D**) PPI network derived from the DEG analysis showing six subnetworks similar to those identified in (**C**). (**E**) PPIs corresponding to genes carrying predicted targets for the miR-106b/93 seed family (red lines) and the miR-25 seed family (blue lines) and showing upregulation between controls and *miR-106b~25* KO testes. Interacting proteins with seeds are represented as black dots whose size is proportional to the number of interactions established. Red and blue interactions are widely distributed throughout the network.

Supplementary Table SIV). Thus, we processed our RNA-seq datasets with the Olego and Quantas pipelines to measure the different types of AS (Wu *et al.*, 2013). We identified 118 AS differences in the mRNAs from 95 genes (Fig. 4A; Supplementary Table SVIII). Sashimi plots confirmed the existence of AS events differing between mutant and control conditions (Fig. 4B–H). Biological processes analysis of the 95 genes with AS differences between conditions identified several groups of genes of particular Gene Ontology categories, including protein poly-ubiquitination, cell cycle and spermatogenesis (Supplementary Table SIX). Overall, our results show that these miRNAs influence not only the abundance but also the sequence of many mature mRNAs, by regulating genes controlling their splicing.

Fertility is not compromised in *miR-106b∼25* KO mice but it is severely reduced in double *miR-17∼92*$^{+/-}$; *miR-106b∼25*$^{-/-}$ mutants

An important aspect of our study was to check whether fertility had been reduced in *miR-106b∼25* KO mice. Fertility tests detected no statistical difference in either the size or the number of the litters (Fig. 5A and B; Supplementary Table SIII). A possible explanation for this is that another factor may be compensating for the lack of *miR-106b∼25*. Several observations indicate that the paralog cluster, *miR-17∼92* is a good candidate: both clusters are expressed in the same cell types during spermatogenesis (Tong *et al.*, 2012); conditional inactivation of *miR-17∼92* in germ cells (Tong *et al.*, 2012) leads to a testicular phenotype similar to that described here for *miR-106b∼25* KO mice; the expression of *miR-106b∼25* is dramatically increased in *miR-17∼92*$^{-/-}$ germ cells (Tong *et al.*, 2012); and likewise, we found that the transcription levels of the *miR-17∼92* host gene increased about 40% in *miR-106b∼25*$^{-/-}$ testes (Fig. 5C; Supplementary Table SII). Hence, we decided to generate compound *miR-17∼92*$^{+/-}$;*miR-106b∼25*$^{-/-}$ mutant mice (hereafter, double knock out: DKO). We could not generate double homozygous mutants because *miR-17∼92*$^{-/-}$ mice die at birth (Ventura *et al.*, 2008). We analyzed these new mutants in the same way as for *miR-106b∼25*$^{-/-}$ mice. At P60, both testis mass and body mass were significantly lower in DKO than in both single mutants (either *miR-106b∼25*$^{-/-}$ or *miR-17∼92*$^{+/-}$) and controls. The relative testis mass reduction in DKO mice was significant compared to the controls, but not regarding the single mutants, owing to their lower body mass (Supplementary Fig. S5A–C). In contrast, the relative seminal vesicle mass showed no difference between any condition (Supplementary Fig. S2 and Supplementary Table SIII). Besides, JSs and the expression patterns of several proteins (cell adhesion molecules and meiotic markers) of both *miR-17∼92*$^{+/-}$ and DKO mutants were similar to those described above for *miR-106b∼25*$^{-/-}$ testes at P60 (Fig. 5D and E; Supplementary Fig. S5D–Q). However, at 12 months of age, *miR-17∼92*$^{+/-}$ mice retained histologically normal testes whereas DKO animals exhibited severe abnormalities, including tubules lacking the seminiferous epithelium and containing only Sertoli cells (Fig. 5F, G and I–L). At P60, the epididymal sperm counts in DKO mice revealed an important reduction compared to any of the other genotypes (Fig. 5H; Supplementary Table SIII). Consistently, we found no differences in fertility between *miR-17∼92*$^{+/-}$ and either control or *miR-106b∼25*$^{-/-}$ mice, but comparison between DKO mice and any of the other three conditions revealed that litter size was reduced in about 35%, and the average number of litters per month per female was reduced in about 75% of mice (Fig. 5A and B; Supplementary Table SIII). Despite this severely reduced fertility detected in DKO mice at P60, they retained some degree of fertility even at the age of 1 year, as their epididymides normally contained sperm (Fig. 5M). However, in a reduced number of cases (2/12), 12-month-old DKO mice were completely sterile, as evidenced by the absolute lack of sperm in their epididymides (Fig. 5N). Altogether, these results indicate that *miR-17∼92* and *miR-106b∼25* co-operate to maintain long-term fertility in the adult testis.

Discussion

The identification of new regulatory genes potentially responsible for the cases of idiopathic male infertility associated with DSD conditions is imperative to meet the diagnostic and therapeutic needs of many of these patients (Lee *et al.*, 2016). The expression of both *miR-106b∼25* and *miR-17∼92* has been shown to be deregulated in several male patients with reproductive defects (Lian *et al.*, 2009; Koster *et al.*, 2010; Wang *et al.*, 2011; Abu-Halima *et al.*, 2016), suggesting that they could be involved in the origin of these disorders. Here, we report that mice with a deletion of *miR-106b∼25* exhibit reduced testis size, altered spermatogenesis and low sperm count and that *miR-17∼92/miR-106b∼25* DKO mice may become completely sterile, showing that these two clusters are necessary to maintain male fertility. Thus, we have identified new candidate genetic factors to be screened in the molecular diagnosis of human males with reproductive disorders.

In our transcriptomic analysis of *miR-106b∼25*-deficient mouse testes, we identified more than 2000 deregulated genes, although most of them showed very mild variations of their expression levels, as observed previously in other tissues and organs (Baek *et al.*, 2008; Selbach *et al.*, 2008). In all cases, including the present study, these modest changes affected not only direct targets but also genes without a predicted binding site in their 3′ UTRs (Han *et al.*, 2015). It seems, therefore, that moderate alteration in the expression of a large number of genes observed in our mutant testes is the result of direct deregulation of a number of target genes, which, in turn, indirectly changes the expression of many other genes functionally related to them. This is consistent with the widely accepted view that miRNAS may act as fine-tuners of large gene networks (Martinez and Walhout, 2009; Han *et al.*, 2015; Rajman and Schratt, 2017). Our results indicate that *miR-106b∼25* miRNAs ensure accurate gene expression in the adult testis by keeping levels within the required thresholds, thus playing a crucial role in testis homeostasis.

Previous studies have shown that members of the *miR-106b∼25* cluster are expressed during early spermatogenesis, from spermatogonial stem cells (SSC) to primary spermatocytes (Hayashi *et al.*, 2008; Niu *et al.*, 2011; McIver *et al.*, 2012; Smorag *et al.*, 2012; Tong *et al.*, 2012; He *et al.*, 2013; Tan *et al.*, 2014; Bhin *et al.*, 2015; Hilz *et al.*, 2017). Consistently, several findings indicate that these early stages are particularly altered in our *miR-106b∼25* KO testes: many genes involved in cell division and mitosis (SSC undergo several mitotic rounds before enter meiosis) are deregulated in mutant testes; the highest number of deregulated genes are those expressed specifically in the cell types of these early stages; and we found a significant increase in the number of DMC1^{+} tubules in the mutant testes, indicating that spermatogenesis is

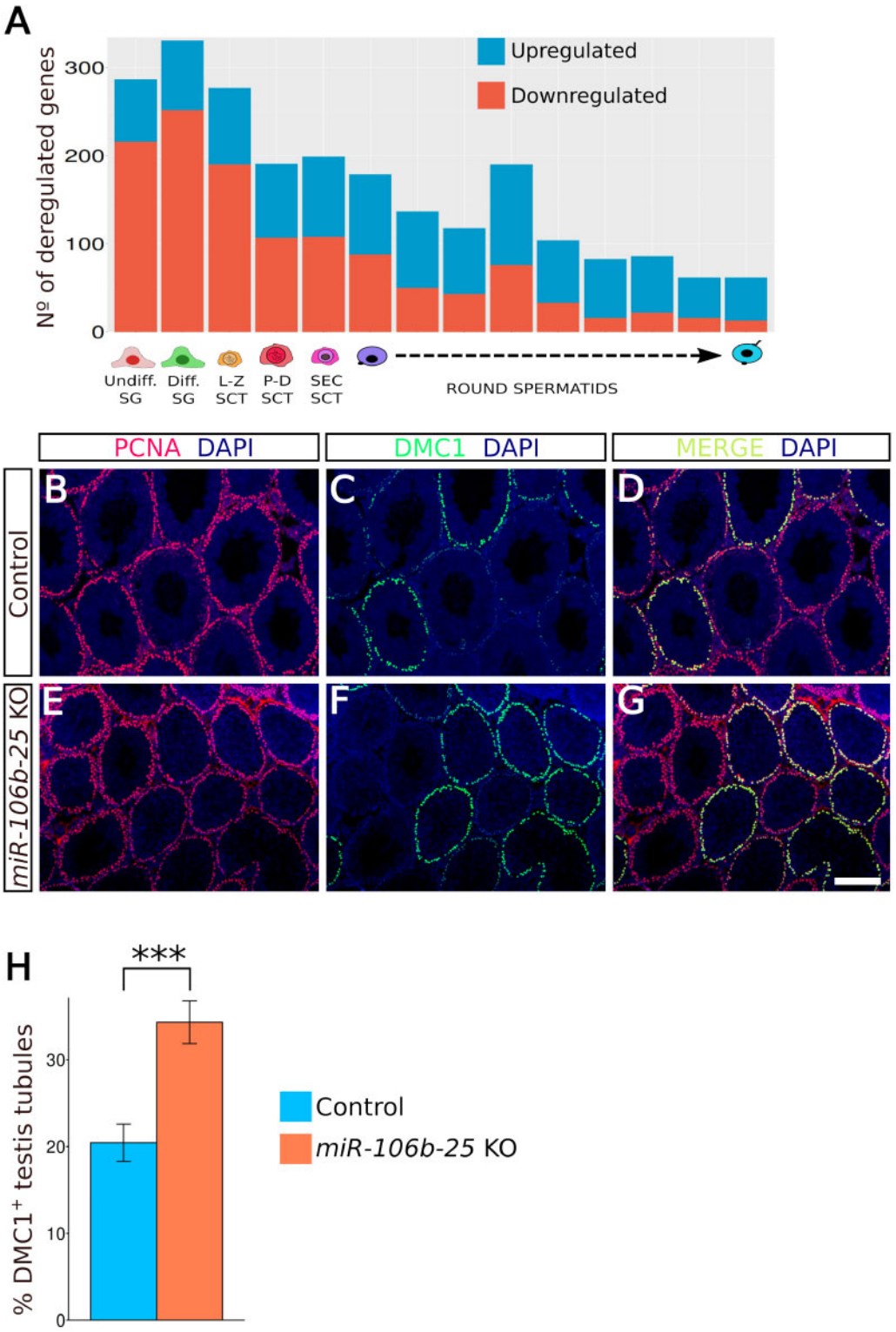

Figure 3 Gene expression alterations and delayed cycle at early spermatogenesis in *miR-106b~25* KO testes at P60. (**A**) Number of genes predicted to be deregulated in each of the cell types of the spermatogenic cycle in *miR-106b~25* KO testes. Most alterations are concentrated in the early stages of the cycle. (**B–G**) Expression pattern of PCNA (mitotic spermatogonia and zygotene-to-pachytene marker) and meiotic recombination protein (DMC1: leptotene-to-early pachytene marker). No differences are seen between control (**B**–**D**) and mutant (**E**–**G**) testes. Color levels of every immunofluorescence micrograph were adjusted as a whole using Gimp. (**H**) Percentage of DMC1-positive seminiferous tubular sections of both control (light blue) and mutant (orange) testes. Bars in (H) represent mean ± SD. Statistical significance of the differences between mean values was determined using Student's *t*-tests; $n = 7$ (3 control and 4 *miR-106b~25* KO mice). All numeric data are included in Supplementary Table SIII. Scale bar shown in (**G**) represents 100 μm in all micrographs.

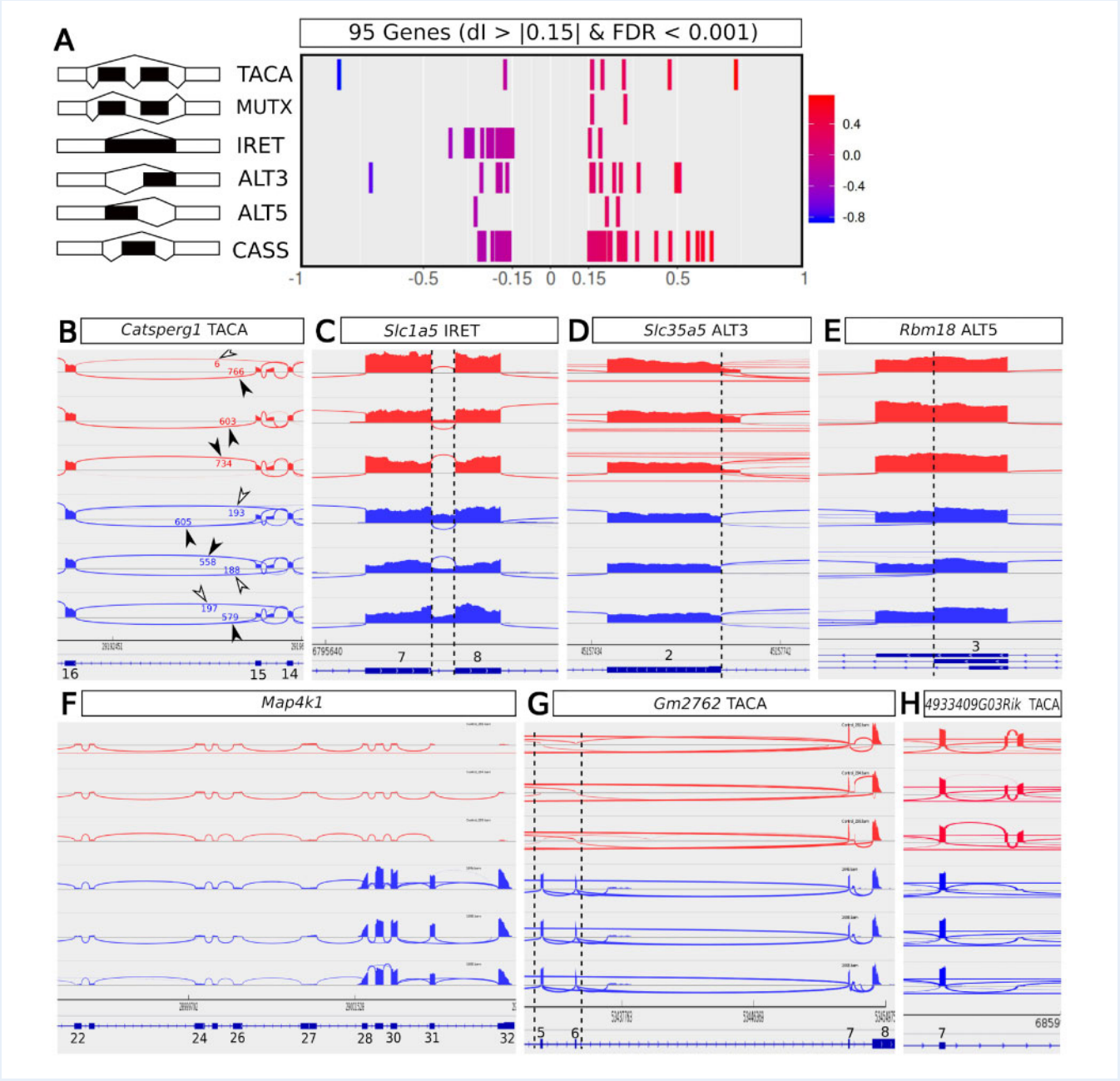

Figure 4 Analysis of mRNA splicing in control and *miR-106b*~*25* KO testes. (**A**) One hundred eighteen AS differences were detected in the mRNAs from 95 genes. The left panel schematically shows the six different types of AS events detected [tandem exons spliced in a coordinated (TACA) or mutually exclusive manner (MUTX), changes in intron retention (IRET), differences in 3′ (ALT3) and 5′ (ALT5) splice site selection, and cassette exons (CASS)]. The right panel shows their differential index of splicing (dI). (**B–H**) Sashimi plots showing several examples of genes with differential splicing events between control (red) and mutant (blue) testes, with indication of the type of AS involved in each case. Exon numbers are shown at the bottom of each panel.

slowed down at the primary spermatocyte stage. Therefore, our results suggest that the absence of *miR-106b*~*25* in the testis causes deregulation of genes involved in cell division that results in a slowing down of spermatogenesis and the subsequent oligozoospermia.

Several studies have reported an increased risk of testicular cancer in infertile men (Jacobsen, 2000; Raman *et al.*, 2005; Walsh *et al.*, 2009; Ji *et al.*, 2012; Eisenberg *et al.*, 2013; Hanson *et al.*, 2016). Although the underlying molecular mechanisms linking the two conditions are poorly understood so far, several considerations are important in the present context: *miR-106b*~*25* members are misregulated in patients with testicular dysfunction (Abu-Halima *et al.*, 2014; Cheng *et al.*, 2017); members of the *miR-106b* seed family have been

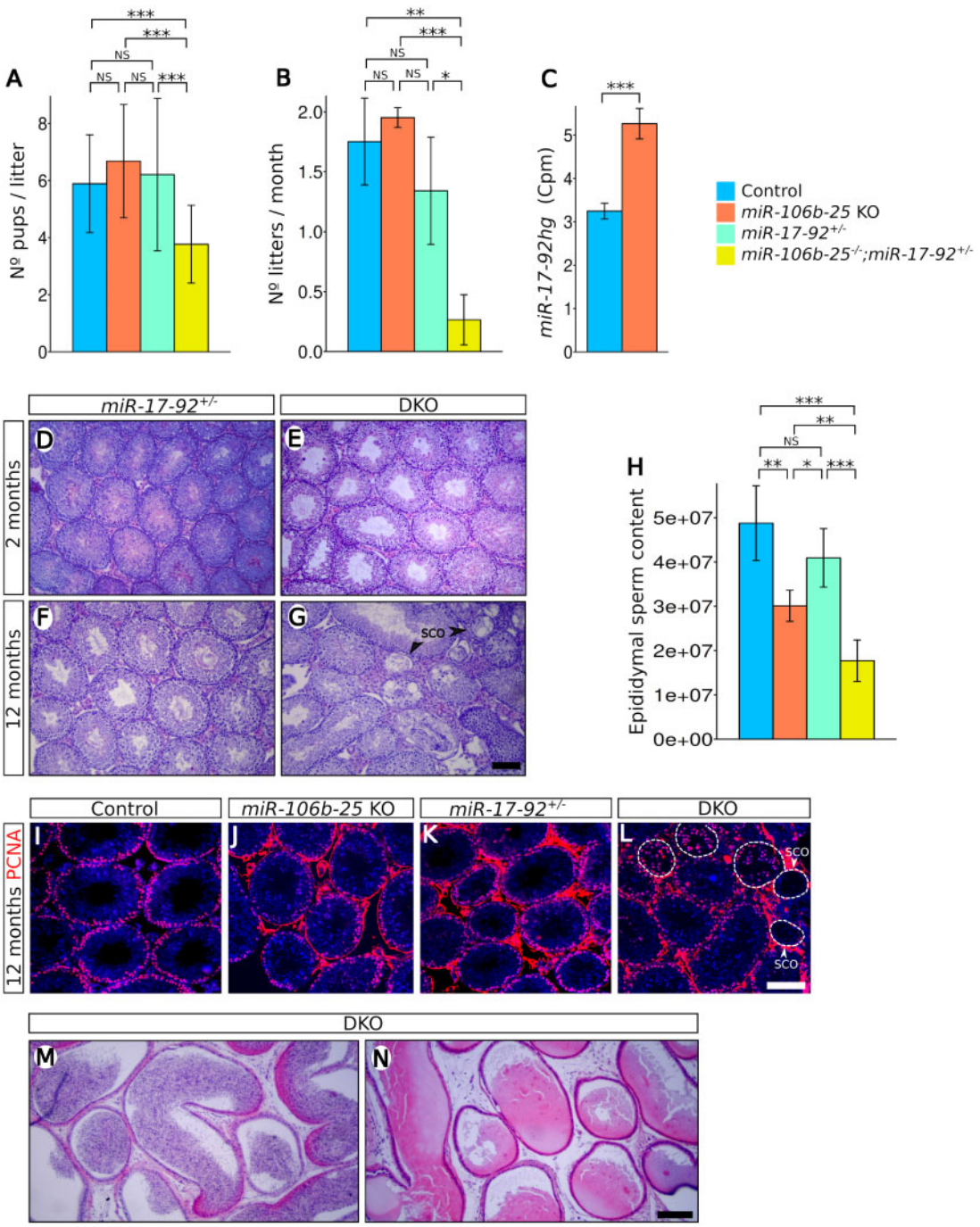

Figure 5 Fertility assessment and testicular phenotype of single *miR-17∼92* and double *miR-17∼92;miR-106b∼25* mutants. Controlled matings were established between either control or mutant mice with control females for a period of 5 months: (**A**) number of pups per litter, (**B**) number of litters per month and per female. (**C**) Expression levels (cpm) of *miR-17∼92hg* (host gene). (**D–G**) Hematoxilin and eosin-stained sections of testes from single (**D** and **F**) and DKO (**E** and **G**) mutants at 2 and 12 months of age; Sertoli cell-only (SCO) seminiferous tubules are present only in 12-month-old, DKO testes. (**H**) Epididymal sperm counts. (**I–L**) PCNA immunofluorescence marking mitotic spermatogonia and zygote-pachytene spermatocytes in control (**I**), *miR-106b∼25* KO (**J**), *miR17∼92* KO (**K**) and DKO testes (**L**) at the age of 12 months. In the DKO testes, degenerating tubules contain just a few positive cells (encircled in white dotted lines) and SCO tubules contain no positive cells. Color levels of every immunofluorescence micrograph were adjusted as a whole using Gimp. **(M and N)** Haematoxilin and eosin-stained sections of the epididymides from two 1-year-old DKO mice: one containing (**M**) and the other lacking (**N**) sperm inside the tubule. Bars in (**A**), (**B**) and (**H**) represent mean ± SD. Statistical significance of the differences between mean values was determined using Student's *t*-tests. FDR < 0.001 in C. $n = 26$ (6 control, 6 *miR-106b∼25* KO, 8 *miR17∼92* KO and 6 DKO mice) in (**A**) and (**B**); $n = 6$ (3 control and 3 *miR-106b∼25* KO mice) in (**C**); $n = 19$ (5 control, 5 *miR-106b∼25* KO, 5 *miR17∼92*$^{+/-}$, and 4 DKO mice) in (**H**). All numeric data are included in Supplementary Table SIII. Scale bar shown in (**G**) represents 100 μm in (**D–G**), the one shown in (**L**) represents 100 μm in (**I–L**) and that shown in (**N**) represents 100 μm in (**M**) and (**N**).

associated with testicular cancer (Koster *et al.*, 2010); the same miRNAs are involved in the control of the cell cycle (Ivanovska *et al.*, 2008; Petrocca *et al.*, 2008); our *miR-106b∼25* KO mice showed altered spermatogenesis and oligozoospermia; and e) the absence of *miR-106b∼25* in the testis leads to the deregulation of many genes involved in cell division and ubiquitination, two processes frequently altered in many types of cancer (Williams and Stoeber, 2012; Mansour, 2018). Hence, *miR-106b∼25* appears to be a good candidate factor connecting the molecular etiologies of both male reproductive disorders and testicular cancer.

RNA mis-splicing is associated with multiple human diseases (Scotti and Swanson, 2016). The testis is one of the organs with a higher number of splicing variants (Soumillon *et al.*, 2013), the majority of AS changes occurring during the mitosis-to-meiosis transition (Hannigan *et al.*, 2017). We found about 40 genes involved in mRNA splicing that were deregulated in *miR-106b∼25* KO testes, some of which are expressed in the germ line during spermatogenesis (Dev *et al.*, 2007; Phillips and Orwig, 2010; Hannigan *et al.*, 2017). Accordingly, we also found 95 genes with AS changes in mutants compared to controls. These genes (Supplementary Table SVIII) are involved in different biological processes such as ubiquitination (*Trim32*, *March8*, *Ubox5*, *Rnf14*), cell cycle (*Ing4*, *Ddx11*, *Hjurp*, *Crocc*, *Foxm1*, *Ppp1cc*) and transport (*Nxt1*, *Slc35c2*, *Cln3*, *Slc1a5*, *Slc9a8*, *Ipo7*, *Ppid*, *Fdxr*, *Slc35a5*, *Magohb*, *Atg16l1* and *Ergic1*). In addition, we also found AS changes in genes with a known role in spermatogenesis, such as *Spo11* (Romanienko and Camerini-Otero, 2000), *Cst8* (Parent *et al.*, 2011) and *Catsperg1* (Wang *et al.*, 2009). Altogether, these results indicate that there is a deregulation of genes involved in mRNA-splicing in *miR-106b-25* KO testes that may cause mis-splicing of a number of genes playing a role in diverse biological processes. This gene network deregulation is probably also partly responsible for the phenotype observed in *miR-106b-25* deficient testes, and provides further evidence of the complexity of the molecular cascade controlled by these miRNAS during testis function.

Our study of DKO mice supported the functional cooperation of *miR-17∼92* and *miR-106b∼25* to maintain fertility. These mice showed more severe spermatogenic alterations and significantly fewer epididymal sperm than simple mutants. More importantly, fertility was severely reduced in DKO mice compared to simple mutants. Fertility decreased with age, as most DKO males are initially fertile (at 2 months) but may become sterile at the age of 1 year. These results demonstrate that both clusters act redundantly in the adult testis. Another interesting feature of DKO mice is their severe idiopathic body mass reduction when compared to controls or simple mutants, a fact that further supports the functional redundancy between both clusters. Their lower vigor might reduce even further their fertility through factors other than sperm production (reduced libido, for instance). In humans, hemizygous deletions of *MIR17HG*, the *miR-17-92* host gene, leads to the Feingold syndrome, characterized by skeletal malformations, but no reproductive anomalies have been described in these patients and familiar cases show that affected individuals may be fertile (de Pontual *et al.*, 2011). In contrast, no human syndrome has been associated with deletions in the *miR-106b-25* cluster, probably because *miR-17-92* may compensate for its absence as we observed in mice.

In summary, here we report that *miR-106b∼25* KO mice show reduced testis size, altered spermatogenesis and oligozoospermia and that, together with *miR-17∼92*, *miR-106b∼25* is necessary to maintain male fertility. Furthermore, taking into account that the two clusters are oncogenic and that patients with reduced fertility are more prone to testicular cancer, our results may also help to elucidate the molecular mechanisms linking both pathologies.

Supplementary data

Supplementary data are available at *Molecular Human Reproduction* online.

Acknowledgements

The authors would like to thank Dr José M. Peinado for helping in serum testosterone determinations.

Authors' roles

F.J.B., M.B. and R.J. conceived the study. A.H., R.P., I.G., M.L., F.M.R., F.D.C., F.J.B. and R.J. performed experiments and analyzed the data. F.J.B. and M.B. performed bioinformatics analysis. A.H., R.P., I.G., F.J.B., M.B. and R.J. discussed and interpreted the results. F.J.B., and R.J. wrote the manuscript. F.J.B. prepared the figures and tables. A.H., I.G. and M.B. reviewed the manuscript. All of the authors read, edited and approved the final version of the manuscript.

Funding

This work was supported by grants from the Andalusian Government, Junta de Andalucía, BIO-109 to R.J. and P11-CVI-7291 to M.B. and grants from the Spanish Ministry of Science and Innovation (CGL2015-67108-P) to R.J. and F.J.B. The authors would like to thank the Spanish Ministry of Science and Innovation for the 'Ramón y Cajal' fellowship granted to F.D.C. (RYC-2014-16458) and the PhD fellowship granted to A.H.

Conflict of interest

The authors declare to have no conflict of interest.

References

Abu-Halima M, Backes C, Leidinger P, Keller A, Lubbad AM, Hammadeh M, Meese E. MicroRNA expression profiles in human testicular tissues of infertile men with different histopathologic patterns. *Fertil Steril* 2014;**101**:78–86.

Abu-Halima M, Ludwig N, Hart M, Leidinger P, Backes C, Keller A, Hammadeh M, Meese E. Altered micro-ribonucleic acid expression profiles of extracellular microvesicles in the seminal plasma of patients with oligoasthenozoospermia. *Fertil Steril* 2016;**106**:1061–1069.

Agarwal V, Bell GW, Nam J-W, Bartel DP. Predicting effective microRNA target sites in mammalian mRNAs. *eLife* 2015;**4**:e05005.

Baek D, Villén J, Shin C, Camargo FD, Gygi SP, Bartel DP. The impact of microRNAs on protein output. *Nature* 2008;**455**:64–71.

Bartel DP. MicroRNAs: genomics, biogenesis, mechanism, and function. *Cell* 2004;**116**:281–297.

Belteki G. Conditional and inducible transgene expression in mice through the combinatorial use of Cre-mediated recombination and tetracycline induction. *Nucleic Acids Res* 2005;**33**:e51.

Bhin J, Jeong H-S, Kim JS, Shin JO, Hong KS, Jung H-S, Kim C, Hwang D, Kim K-S. PGC-enriched miRNAs control germ cell development. *Mol Cells* 2015;**38**:895–903.

Cheng YS, Chung CL, Chen CF, Lin YM. Differential expression of microRNAs and their messengerRNA targets in men with normal spermatogenesis versus Sertoli cell-only syndrome. *Urol Sci* 2017;**28**:42–49.

Dadhich RK, Barrionuevo FJ, Real FM, Lupiañez DG, Ortega E, Burgos M, Jiménez R. Identification of live germ-cell desquamation as a major mechanism of seasonal testis regression in mammals: a study in the iberian mole (*Talpa occidentalis*). *Biol Reprod* 2013;**88**:1–12.

de Pontual L, Yao E, Callier P, Faivre L, Drouin V, Cariou S, Van Haeringen A, Geneviève D, Goldenberg A, Oufadem M *et al*. Germline deletion of the miR-17∼92 cluster causes skeletal and growth defects in humans. *Nat Genet* 2011;**43**:1026–1030.

Dev A, Nayernia K, Meins M, Adham I, Lacone F, Engel W. Mice deficient for RNA-binding protein brunol1 show reduction of spermatogenesis but are fertile. *Mol Reprod Dev* 2007;**74**:1456–1464.

Eisenberg ML, Betts P, Herder D, Lamb DJ, Lipshultz LI. Increased risk of cancer among azoospermic men. *Fertil Steril* 2013;**100**:681–685.

Guarnieri AL, Towers CG, Drasin DJ, Oliphant MUJ, Andrysik Z, Hotz TJ, Vartuli RL, Linklater ES, Pandey A, Khanal S *et al*. The miR-106b-25 cluster mediates breast tumor initiation through activation of NOTCH1 via direct repression of NEDD4L. *Oncogene* 2018;**37**:3879–3893.

Han Y-C, Vidigal JA, Mu P, Yao E, Singh I, González AJ, Concepcion CP, Bonetti C, Ogrodowski P, Carver B *et al*. An allelic series of miR-17∼92–mutant mice uncovers functional specialization and cooperation among members of a microRNA polycistron. *Nat Genet* 2015;**47**:766–775.

Hannigan MM, Zagore LL, Licatalosi DD. Ptbp2 controls an alternative splicing network required for cell communication during spermatogenesis. *Cell Rep* 2017;**19**:2598–2612.

Hanson HA, Anderson RE, Aston KI, Carrell DT, Smith KR, Hotaling JM. Subfertility increases risk of testicular cancer: evidence from population-based semen samples. *Fertil Steril* 2016;**105**:322–328.

Hayashi K, Chuva de Sousa Lopes SM, Kaneda M, Tang F, Hajkova P, Lao K, O'Carroll D, Das PP, Tarakhovsky A, Miska EA *et al*. MicroRNA biogenesis is required for mouse primordial germ cell development and spermatogenesis. *PLoS One* 2008;**3**:e1738.

He Z, Jiang J, Kokkinaki M, Tang L, Zeng W, Gallicano I, Dobrinski I, Dym M. MiRNA-20 and mirna-106a regulate spermatogonial stem cell renewal at the post-transcriptional level via targeting STAT3 and Ccnd1: spermatogonial stem cell regulation by microRNAs. *Stem Cells* 2013;**31**:2205–2217.

Hermann BP, Cheng K, Singh A, Roa-De La Cruz L, Mutoji KN, Chen I-C, Gildersleeve H, Lehle JD, Mayo M, Westernströer B *et al*. The mammalian spermatogenesis single-cell transcriptome, from spermatogonial stem cells to spermatids. *Cell Rep* 2018;**25**:1650–1667.e8.

Hilz S, Fogarty EA, Modzelewski AJ, Cohen PE, Grimson A. Transcriptome profiling of the developing male germ line identifies the miR-29 family as a global regulator during meiosis. *RNA Biol* 2017;**14**:219–235.

Huang DW, Sherman BT, Tan Q, Kir J, Liu D, Bryant D, Guo Y, Stephens R, Baseler MW, Lane HC *et al*. DAVID Bioinformatics Resources: expanded annotation database and novel algorithms to better extract biology from large gene lists. *Nucleic Acids Res* 2007;**35**:W169–W175.

Hudson RS, Yi M, Esposito D, Glynn SA, Starks AM, Yang Y, Schetter AJ, Watkins SK, Hurwitz AA, Dorsey TH *et al*. MicroRNA-106b-25 cluster expression is associated with early disease recurrence and targets caspase-7 and focal adhesion in human prostate cancer. *Oncogene* 2013;**32**:4139–4147.

Ivanovska I, Ball AS, Diaz RL, Magnus JF, Kibukawa M, Schelter JM, Kobayashi SV, Lim L, Burchard J, Jackson AL *et al*. MicroRNAs in the miR-106b family regulate p21/CDKN1A and promote cell cycle progression. *Mol Cell Biol* 2008;**28**:2167–2174.

Jacobsen R. Risk of testicular cancer in men with abnormal semen characteristics: cohort study. *BMJ* 2000;**321**:789–792.

Ji G, Long Y, Zhou Y, Huang C, Gu A, Wang X. Common variants in mismatch repair genes associated with increased risk of sperm DNA damage and male infertility. *BMC Med* 2012;**10**:49.

Johnsen SG. Testicular biopsy score count—a method for registration of spermatogenesis in human testes: normal values and results in 335 hypogonadal males. *Horm Res Paediatr* 1970;**1**:2–25.

Koster R, di Pietro A, Timmer-Bosscha H, Gibcus JH, van den Berg A, Suurmeijer AJ, Bischoff R, Gietema JA, de Jong S. Cytoplasmic p21 expression levels determine cisplatin resistance in human testicular cancer. *J Clin Invest* 2010;**120**:3594–3605.

Lee PA, Houk CP, Ahmed SF, Hughes IA. Consensus statement on management of intersex disorders. *Pediatrics* 2006;**118**:e488–e500.

Lee PA, Nordenström A, Houk CP, Ahmed SF, Auchus R, Baratz A, Dalke KB, Liao L-M, Lin-Su K, Looijenga LH 3rd. Global disorders of sex development update since 2006: perceptions, approach and care. *Horm Res Paediatr* 2016;**85**:158–180.

Li Y, Tan W, Neo TWL, Aung MO, Wasser S, Lim SG, Tan TMC. Role of the miR-106b-25 microRNA cluster in hepatocellular carcinoma. *Cancer Sci* 2009;**100**:1234–1242.

Lian J, Zhang X, Tian H, Liang N, Wang Y, Liang C, Li X, Sun F. Altered microRNA expression in patients with non-obstructive azoospermia. *Reprod Biol Endocrinol* 2009;**7**:13.

Liao Y, Smyth GK, Shi W. The R package Rsubread is easier, faster, cheaper and better for alignment and quantification of RNA sequencing reads. *Nucleic Acids Res* 2019;**47**:e47.

Lo Sardo F, Forcato M, Sacconi A, Capaci V, Zanconato F, Di Agostino S, Del Sal G, Pandolfi PP, Strano S, Bicciato S *et al*. MCM7 and its hosted miR-25, 93 and 106b cluster elicit YAP/TAZ oncogenic activity in lung cancer. *Carcinogenesis* 2017;**38**:64–75.

Lui W-Y, Cheng CY. Transcriptional regulation of cell adhesion at the blood-testis barrier and spermatogenesis in the testis. In: CY Cheng (ed). *Biology and Regulation of Blood-Tissue Barriers*. Vol. **763**. New York, NY: Springer New York, 2013, 281–294.

Mansour MA. Ubiquitination: friend and foe in cancer. *Int J Biochem Cell Biol* 2018;**101**:80–93.

Martinez NJ, Walhout AJM. The interplay between transcription factors and microRNAs in genome-scale regulatory networks. *BioEssays* 2009;**31**:435–445.

McIver SC, Stanger SJ, Santarelli DM, Roman SD, Nixon B, McLaughlin EA. A unique combination of male germ cell miRNAs coordinates gonocyte differentiation. *PLoS One* 2012;**7**:e35553.

Mogilyansky E, Rigoutsos I. The miR-17/92 cluster: a comprehensive update on its genomics, genetics, functions and increasingly important and numerous roles in health and disease. *Cell Death Differ* 2013;**20**:1603–1614.

Niu Z, Goodyear SM, Rao S, Wu X, Tobias JW, Avarbock MR, Brinster RL. MicroRNA-21 regulates the self-renewal of mouse spermatogonial stem cells. *Proc Natl Acad Sci USA* 2011;**108**:12740–12745.

Parent AD, Cornwall GA, Liu LY, Smith CE, Hermo L. Alterations in the testis and epididymis associated with loss of function of the cystatin-related epididymal spermatogenic (CRES) protein. *J Androl* 2011;**32**:444–463.

Petrocca F, Visone R, Onelli MR, Shah MH, Nicoloso MS, de Martino I, Iliopoulos D, Pilozzi E, Liu C-G, Negrini M *et al*. E2F1-regulated microRNAs impair TGFβ-dependent cell-cycle arrest and apoptosis in gastric cancer. *Cancer Cell* 2008;**13**:272–286.

Phillips BT, Orwig KE. Regulation of the RNA binding protein YBX1 in mouse undifferentiated spermatogonia. *Biol Reprod* 2010;**83**:407.

Rajman M, Schratt G. MicroRNAs in neural development: from master regulators to fine-tuners. *Development* 2017;**144**:2310–2322.

Raman JD, Nobert CF, Goldstein M. Increased incidence of testicular cancer in men presenting with infertility and abnormal semen analysis. *J Urol* 2005;**174**:1819–1822.

Robinson JT, Thorvaldsdóttir H, Winckler W, Guttman M, Lander ES, Getz G, Mesirov JP. Integrative genomics viewer. *Nat Biotechnol* 2011;**29**:24–26.

Robinson MD, McCarthy DJ, Smyth GK. edgeR: a Bioconductor package for differential expression analysis of digital gene expression data. *Bioinformatics* 2010;**26**:139–140.

Romanienko PJ, Camerini-Otero RD. The mouse Spo11 gene is required for meiotic chromosome synapsis. *Mol Cell* 2000;**6**:975–987.

Scotti MM, Swanson MS. RNA mis-splicing in disease. *Nat Rev Genet* 2016;**17**:19–32.

Selbach M, Schwanhäusser B, Thierfelder N, Fang Z, Khanin R, Rajewsky N. Widespread changes in protein synthesis induced by microRNAs. *Nature* 2008;**455**:58–63.

Shannon P. Cytoscape: a software environment for integrated models of biomolecular interaction networks. *Genome Res* 2003;**13**:2498–2504.

Smorag L, Zheng Y, Nolte J, Zechner U, Engel W, Pantakani DVK. MicroRNA signature in various cell types of mouse spermatogenesis: evidence for stage-specifically expressed miRNA-221, -203 and -34b-5p mediated spermatogenesis regulation. *Biol Cell* 2012;**104**:677–692.

Soumillon M, Necsulea A, Weier M, Brawand D, Zhang X, Gu H, Barthès P, Kokkinaki M, Nef S, Gnirke A *et al*. Cellular source and mechanisms of high transcriptome complexity in the mammalian testis. *Cell Rep* 2013;**3**:2179–2190.

Steger K. The proliferation of spermatogonia in normal and pathological human seminiferous epithelium: an immunohistochemical study using monoclonal antibodies against Ki-67 protein and proliferating cell nuclear antigen. *Mol Hum Reprod* 1998;**4**:227–233.

Szklarczyk D, Gable AL, Lyon D, Junge A, Wyder S, Huerta-Cepas J, Simonovic M, Doncheva NT, Morris JH, Bork P *et al*. STRING v11: protein–protein association networks with increased coverage, supporting functional discovery in genome-wide experimental datasets. *Nucleic Acids Res* 2019;**47**:D607–D613.

Tan T, Zhang Y, Ji W, Zheng P. miRNA signature in mouse spermatogonial stem cells revealed by high-throughput sequencing. *BioMed Res Int* 2014;**2014**:1–11.

Tong M-H, Mitchell DA, McGowan SD, Evanoff R, Griswold MD. Two miRNA clusters, Mir-17-92 (Mirc1) and Mir-106b-25 (Mirc3), are involved in the regulation of spermatogonial differentiation in mice. *Biol Reprod* 2012;**86**:72.

Ventura A, Young AG, Winslow MM, Lintault L, Meissner A, Erkeland SJ, Newman J, Bronson RT, Crowley D, Stone JR *et al*. Targeted deletion reveals essential and overlapping functions of the miR-17 through 92 family of miRNA clusters. *Cell* 2008;**132**:875–886.

Walsh TJ, Croughan MS, Schembri M, Chan JM, Turek PJ. Increased risk of testicular germ cell cancer among infertile men. *Arch Intern Med* 2009;**169**:351–356.

Wang C, Yang C, Chen X, Yao B, Yang C, Zhu C, Li L, Wang J, Li X, Shao Y *et al*. Altered profile of seminal plasma microRNAs in the molecular diagnosis of male infertility. *Clin Chem* 2011;**57**:1722–1731.

Wang H, Liu J, Cho K-H, Ren D. A novel, single, transmembrane protein CATSPERG is associated with CATSPER1 channel protein. *Biol Reprod* 2009;**81**:539–544.

Williams GH, Stoeber K. The cell cycle and cancer. *J Pathol* 2012;**226**:352–364.

Wu J, Anczuków O, Krainer AR, Zhang MQ, Zhang C. OLego: fast and sensitive mapping of spliced mRNA-Seq reads using small seeds. *Nucleic Acids Res* 2013;**41**:5149–5163.

Xiang W, He J, Huang C, Chen L, Tao D, Wu X, Wang M, Luo G, Xiao X, Zeng F *et al*. miR-106b-5p targets tumor suppressor gene SETD2 to inactive its function in clear cell renal cell carcinoma. *Oncotarget* 2015;**6**:4066–4079.

Yan Q, Weyn-Vanhentenryck SM, Wu J, Sloan SA, Zhang Y, Chen K, Wu JQ, Barres BA, Zhang C. Systematic discovery of regulated and conserved alternative exons in the mammalian brain reveals NMD modulating chromatin regulators. *Proc Natl Acad Sci USA* 2015;**112**:3445–3450.

Yoshida K, Kondoh G, Matsuda Y, Habu T, Nishimune Y, Morita T. The mouse RecA-like gene Dmc1 is required for homologous chromosome synapsis during meiosis. *Mol Cell* 1998;**1**:707–718.

Zhang B, Wang Q, Pan X. MicroRNAs and their regulatory roles in animals and plants. *J Cell Physiol* 2007;**210**:279–289.

Zhang R, Wang W, Li F, Zhang H, Liu J. MicroRNA-106b~25 expressions in tumor tissues and plasma of patients with gastric cancers. *Med Oncol* 2014;**31**:243.

Zhu Z. MiR-25 regulates apoptosis by targeting Bim in human ovarian cancer. *Oncol Rep* 2012;**27**:594–598.